Title	Transient receptor potential canonical 3 inhibitor Pyr3 improves outcomes and attenuates astrogliosis after intracerebral hemorrhage in mice.
Author(s)	Munakata, Masaya; Shirakawa, Hisashi; Nagayasu, Kazuki; Miyanohara, Jun; Miyake, Takahito; Nakagawa, Takayuki; Katsuki, Hiroshi; Kaneko, Shuji
Citation	Stroke (2013), 44(7): 1981-1987
Issue Date	2013-07
URL	http://hdl.handle.net/2433/187123
Right	© 2013 American Heart Association, Inc.
Type	Journal Article
Textversion	author

Original Contribution

The TRPC3 inhibitor Pyr3 improves outcomes and attenuates astrogliosis after intracerebral hemorrhage in mice

Masaya Munakata MS; Hisashi Shirakawa, PhD; Kazuki Nagayasu, PhD; Jun Miyanohara BS; Takahito Miyake BS; Takayuki Nakagawa, PhD; Hiroshi Katsuki, PhD; Shuji Kaneko, PhD

From Department of Molecular Pharmacology, Graduate School of Pharmaceutical Sciences, Kyoto University (M.M., H.S., K.N., J.M., T.M., T.N., S.K.,) and Department of Chemico-Pharmacological Sciences, Graduate School of Pharmaceutical Sciences, Kumamoto University (H.K.,).

Correspondence to:

Shuji Kaneko, PhD;

Department of Molecular Pharmacology, Graduate School of Pharmaceutical Sciences, Kyoto University. 46-29 Yoshida-shimoadachi-cho, Sakyo-ku, Kyoto, 606-8501, Japan,

Tel: +81-75-753-4541; Fax: +81-75-753-4542; E-mail; skaneko@pharm.kyoto-u.ac.jp

Cover title: Protective effect of TRPC3 inhibition against ICH

Number of figures: 6; supplementary figures: 4; tables: 0 ; words: 5012

Keywords: intracerebral hemorrhage, inflammation, astrocyte, TRPC channel, TRPC3, Pyr3,

Subject code: [43] Acute Cerebral Hemorrhage

Abstract

Background and purpose: Intracerebral hemorrhage (ICH) stems from the rupture of blood vessels in the brain, with the subsequent accumulation of blood in the parenchyma. Increasing evidence suggests that blood-derived factors induce excessive inflammatory responses that are involved in the progression of ICH-induced brain injury. Thrombin, a major blood-derived factor, leaks into the brain parenchyma upon blood-brain barrier (BBB) disruption and induces brain injury and astrogliosis. Furthermore, thrombin dynamically upregulates transient receptor potential canonical 3 (TRPC3) channel, which contributes to pathological astrogliosis through a feed-forward upregulation of its own expression. The present study investigated whether Pyr3, a specific TRPC3 inhibitor, can improve functional outcomes and attenuate astrogliosis after ICH in mice.

Methods: Male C57BL6 mice received an intracerebral infusion of collagenase or autologous blood to induce ICH. Pyr3 was given both intracerebroventricularly and intraperitoneally after ICH induction. ICH-induced brain injury was evaluated by quantitative assessment of neurological deficits, brain swelling and injury volume after ICH. Astrocyte activation was evaluated by immunohistochemical assessment of changes in S100 protein expression.

Results: Neurological deficits, neuronal injury, brain edema, and astrocyte activation were all significantly improved by administration of Pyr3. Moreover, delayed administration of Pyr3 at 6 h or 1 day following blood or collagenase infusion, respectively, also improved the symptoms.

Conclusions: Pyr3, a specific inhibitor of TRPC3, reduced the perihematomal accumulation of astrocytes and ameliorated ICH-induced brain injury. Therefore, TRPC3 provides a new therapeutic target for the treatment of hemorrhagic brain injury.

Introduction

Intracerebral hemorrhage (ICH) is a subtype of stroke with high morbidity and mortality.[1] Although several therapeutic strategies for management of ICH are currently in clinical practice,[1] virtually none are aimed at neuroprotection. Basic researches have demonstrated that various drugs that possess antioxidative, anti-inflammatory or neurotrophic/neuroprotective properties produce therapeutic effects on ICH animal models,[2, 3] however effective drug therapies for ICH are yet unavailable.

Modulation of inflammatory processes mediated by astrocytes, neutrophils, and so on may provide an opportunity for restricting the expansion of ICH-induced tissue damage.[3,4] Astrocytes accumulate in the perihematomal region[5] and induce toxic edema, provoke inflammation, release cytotoxins, and form scars following ICH.[6] Moreover, neutrophils, macrophages, and microglia are major central nervous system sources of cytokines, chemokines, and other immunomolecules[4] and are thought to provoke secondary brain damage after ICH.

Transient receptor potential (TRP) channels are formed by homomeric or heteromeric tetramers of six subtypes of TRP proteins that constitute six subfamilies: the TRP-ankyrin transmembrane protein 1 (TRPA1), TRP-canonical (TRPC), TRP-melastatin (TRPM), TRP-mucolipin (TRPML), TRP-polycystin (TRPP), and TRP-vanilloid (TRPV) subfamilies.[7] There are seven TRPC channel isoforms that function as homotetrameric or heterotetrameric cation channels. At least one isoform is expressed in almost every tissue, where it facilitates voltage-independent Ca^{2+} entry in response to calcium store depletion induced by receptor stimulation.[8] TRPC3 channels

are directly activated by diacylglycerol[9] and underlie the store-operated channels observed in many cell types. We previously showed that thrombin, a predominant blood-derived factor, induced functional activation of astrocytes via opening of the TRPC3 channel in human astrocytoma cell lines[10] and rat cultured astrocytes.[11] Although systemic administration of argatroban, a direct thrombin inhibitor, significantly reduced brain edema after ICH,[12] the effect of TRPC3 inhibition *per se* has not yet been clarified in an *in vivo* model of ICH.

In the present study, we investigated whether Pyr3, a selective TRPC3 inhibitor, would attenuate brain injury and inflammatory response after in the collagenase/autologous blood infusion mouse models of ICH.[13] It is clearly demonstrated that Pyr3 directly binds TRPC3 channel protein, selectively inhibits TRPC3 channel activity and can improve TRPC3-related diseases such as cardiac hypertrophy.[14] In addition, Pyr3 reduced Ca^{2+} responses in wild-type acini to the same extent as deletion of Trpc3 and had no effect on the Ca^{2+} signal in $Trpc3^{-/-}$ acini,[15] suggesting that Pyr3 is a useful tool for clarification of TRPC3 functions and for treatments of TRPC3-mediated diseases. Our data suggest that TRPC3 is involved in the development of brain injury after ICH, implicating TRPC3 as a new therapeutic target for the prevention of secondary brain injury and neurological deficits after stroke.

Materials and methods

Induction of ICH and Pyr3 treatment

All experiments were conducted in accordance with the ethical guidelines of the Kyoto University Animal Research Committee. Male C57BL/6J mice (8–13 weeks of age) weighing 21–28 g were used to produce the collagenase[3] and autologous blood infusion ICH models.[16] Animals were maintained at constant ambient temperature (22°C ± 1°C) under a 12 h light/dark cycle. After intraperitoneal injection of 50 mg/kg pentobarbital, mice were placed in a stereotaxic frame. A 30-gauge needle was inserted through a burr hole on the skull into the striatum (stereotaxic coordinates: 2.3 mm lateral to the midline, 0.2 mm anterior to the bregma, and 3.5 mm below the skull). In the collagenase infusion model, ICH was induced by microinfusion pump-mediated injection of 0.025 U collagenase type VII (Sigma, MO, USA) in 0.5 μL phosphate buffered saline (PBS) at a constant rate of 0.20 μL/min. In the autologous blood infusion model, ICH was induced by injection of 5 μL autologous blood from the tail vein at a constant rate of 2 μL/min. The injection was terminated and 2.5 min later, 10 μL autologous blood was injected at a constant rate of 2 μL/min. Body temperature was measured with a rectal probe and maintained at 37°C after surgery.

Pyr3 was suspended in 10% HCO-60 at a concentration of 4 mmol/L and intracerebroventricularly administered just one time at a concentration of 1, 10, or 20 nmol/5 μL at 5 min after the induction of ICH. Thereafter, Pyr3 was intraperitoneally administered at a concentration of 2, 20, or 40 mg/kg, twice per day unless otherwise

noted. In post-treatment studies, intracerebroventricular administration of Pyr3 was performed at 24 or 48 h after collagenase injection or at 6 h after blood injection, followed by intraperitoneal administration. **The mice were randomly assigned to receive vehicle alone or varying doses of Pyr3. All behavioral and histological experiments and their subsequent evaluation were performed by an experimenter blinded to the identity of the treatment groups.**

Behavioral Tests

Neurological and sensorimotor functions were evaluated via the neurological deficit scoring (NDS) system, rotarod test, and rope grip test at 1, 3, and 7 days after surgery.

In the NDS system, mice were scored by using a 28-point NDS system.[17] The tests included body symmetry, gait, climbing, circling behavior, front limb symmetry, compulsory circling, and whisker response. Each point was graded from 0 to 4. Maximum deficit score was 28.

In the rotarod test, mice were placed on a rotarod cylinder, and the duration for which the mouse remained on the rotarod was recorded. The rotation speed was slowly increased from 4–40 revolutions/min within a period of 3 min. The trial was ended if the animal fell off the rotarod or gripped the device and spun around for two or more consecutive revolutions. Animals were trained in advance before induction of ICH.

In the rope grip test, mice were placed midway on a string between two supports and rated as follows: 0, falls off; 1, hangs onto string by one or both forepaws; 2, same as for 1, but attempts to climb onto string; 3, hangs onto string by one or both forepaws

plus one or both hind paws; 4, hangs onto string by forepaws and hind paws plus tail wrapped around string; and 5, escapes to the supports.[18] The final score was the average of five trials.

Hemorrhagic injury and hemispheric enlargement analysis

Twenty micrometer coronal sections were cut with a cryostat and stored at −80°C prior to staining with Nissl. Sections were digitized and analyzed with the use of Image J software. The hemorrhagic injury area was calculated by quantifying the Nissl staining-negative area in each section, and the hemorrhagic injury volume was computed by summation of the Nissl staining-negative areas multiplied by the interslice distance (200 μm). Brain edema was measured on the basis of hemispheric enlargement at the bregma, which was calculated according to the following formula: [(ipsilateral hemisphere volume − contralateral hemisphere volume)/contralateral hemisphere volume] × 100%.

Immunohistochemistry

Three days after ICH, mice were anesthetized with pentobarbital and perfused transcardially with PBS (10 mL), followed by 4% paraformaldehyde (10 mL). Brains were isolated and fixed in 4% paraformaldehyde for 3 h and then soaked in 15% sucrose overnight at 4°C. After freezing, brains were cut into 20 μm thick sections, and five sections around the injection site were collected every 200 μm and mounted onto slides. After rinsing with PBS containing 0.1% Triton X-100 (tPBS), specimens were treated

with tPBS-containing blocking serum for 1 h at room temperature and then incubated with rabbit anti-S100 antibody (1:400, Dako, Tokyo, Japan), rabbit anti-Iba1 antibody (1:500, Wako, Osaka, Japan) and rat anti Gr1/Ly6G antibody (1:300, R&D Systems, MN, USA) overnight at 4°C. After rinsing with PBS, specimens were incubated with Alexa Fluor 594 donkey anti-rabbit IgG (1:200, Invitrogen, CA, USA) or Alexa Fluor 594 goat anti-rat IgG (1:200 Invitrogen) for 1 h at room temperature. The average number of S100 and Iba1-positive cells at the perihematomal area and Gr1-positive cells in the hematoma per 640 × 640 μm^2 was counted for at least two independent sections. Confocal images were obtained by using a Fluoview FV10i system (Olympus, Tokyo, Japan).

Statistical Analysis

Data are presented as the mean ± the SD. For comparisons among multiple groups, one-way or two-way analysis of variance followed by a post hoc Bonferroni test was used to determine significant differences. Differences between two groups were assessed with the Student's t-test. Statistical significance was set at $P < 0.05$.

Results

Effect of Pyr3 on hematoma formation and neurological deficits in the collagenase infusion ICH model

ICH is accompanied by hematoma formation and characteristic behavioral deficits. To assess whether Pyr3 affects hematoma formation, we first compared the size of hematomas in vehicle and Pyr3-treated mice at 6 h after the induction of ICH in the striatum by collagenase injection. No difference was observed in hematoma formation between groups (Fig. 1A). To evaluate whether Pyr3 influenced recovery from neurologic deficits, various behavioral experiments were conducted. As a result, the NDS of vehicle-treated mice was found to increase substantially at 1–7 days after collagenase injection. Pyr3 administration substantially improved the NDS at all time points examined (Fig. 1B).

In the rotarod test, induction of ICH resulted in substantial performance deficits in vehicle-treated mice, as indicated by a decrease in the latency to fall. Pyr3 treatment significantly prevented the decrease at 3 days after ICH (Fig. 1C). A decrease in rope climbing performance was also evident after ICH in the rope grip test, but Pyr3 treatment had a tendency to improve the test score (Fig. 1D). Pyr3 administration alone did not cause any neurological adverse effect including gait abnormality (data not shown), unlike the previous data in TRPC3-deficient mice.[19]

Effect of Pyr3 on ICH-induced neuronal loss and brain edema

The effect of Pyr3 was evaluated in relation to the hemorrhagic injury volume and hemispheric enlargement of the injured brain, which both increased after ICH due to neuronal loss and brain edema, respectively. Pyr3 prevented the increase in hemorrhagic injury volume (Fig. 2A–C) and hemispheric enlargement (Fig. 2D) at 3 days after injury.

Intracerebrovebtricular vs. intraperitoneal administration of Pyr3

Next, we evaluated the efficacy of intraperitoneal vs. intracerebroventricular administration of Pyr3 for treatment of ICH. Intracerebroventricular administration alone had a tendency to improve motor function in the rotarod or rope grip test but not intraperitoneal alone (Supplementary Fig. 1B, C). On the other hand, both the NDS and hemorrhagic injury volume were slightly but significantly improved at day 3 after ICH (Supplementary Fig. 1A, D). However, the best protection was afforded by the combined intraperitoneal/intracerebroventricular route. Therefore, this method of Pyr3 administration was employed for the remainder of the study.

Concentration-dependent actions of Pyr3

The concentration-dependence of Pyr3 was next examined following combined intracerebroventricular/intraperitoneal administration of the drug (1, 10, or 20 nmol/5 µl intracerebroventricular, and 2, 20, or 40 mg/kg intraperitoneal). The lowest drug dose (1 nmol/5 µl intracerebroventricular and 2 mg/kg intraperitoneal) yielded no significant differences between vehicle and Pyr3-treated mice (Fig. 3). However, the hemorrhagic

injury volume, NDS, running performance in the rotarod test, and rope grip score were all improved in a concentration-dependent manner.

Delayed administration of Pyr3

To assess the therapeutic time window for Pyr3 administration, Pyr3 was administered to mice at 1 or 2 days after ICH induction. Drug administration at 2 days after ICH did not protect mice against ICH-induced injury; however, drug administration at 1 day after ICH significantly decreased hemorrhagic injury volume and the NDS, and had a tendency to improve motor function in the rotarod and rope grip test (Fig. 4).

Reduction in perihematomal accumulation of astrocytes in Pyr3-treated mice

We have previously shown that TRPC3 contributes to pathological activation of astrocytes. To investigate the influence of TRPC3 inhibition on astrocyte behavior *in vivo*, we examined the perihematomal accumulation of activated astrocytes at 1, 3, and 7 days after ICH via immunohistochemical staining for S100 protein. The number of S100-positive astrocytes in the perihematomal area was increased at 1 day after ICH and remained elevated throughout the course of the experiment, whereas Pyr3 partially prevented the increase (Fig. 5A, B). Moreover, we assessed the accumulation of microglia/macrophages and neutrophils using by anti-Iba1 and anti-Gr1 antibodies, respectively, at 1, 3, and 7 days after ICH. The number of Iba1-positive cells in the perihematomal area was increased after ICH and peaked at 3-7 days after ICH, which was significantly inhibited in that of Pyr3-treated mice (Supplementary Fig. 2). The

number of Gr1-positive cells in the hematoma was increased after ICH and peaked at 1 day after ICH, whereas they did not appear at 7 days. There was no **difference** in the number of Gr1-positive cells between vehicle and Pyr3-treated group (Supplementary Fig. 3).

Effect of Pyr3 in the autologous blood infusion ICH model

We next investigated the actions of Pyr3 in the autologous blood infusion ICH model. Hematoma formation was comparable between vehicle and Pyr3-treated mice at 6 h after ICH (Fig. 6A). The NDS increased in vehicle-treated mice after autologous blood infusion, but Pyr3 treatment significantly prevented the increase (Fig. 6B). In the rotarod and rope grip tests, induction of ICH in vehicle-treated mice resulted in a substantial decline in performance (Fig. 6B). This decline was also prevented by Pyr3 (Fig. 6B).

Furthermore, the therapeutic time window for Pyr3 administration after autologous blood infusion was assessed by administration of the drug at 6 h after ICH. Even such delayed administration of Pyr3 significantly decreased the NDS at 24 and 72 h after ICH and significantly increased the rope grip test score at 24 h (Fig. 6C).

Moreover, the distribution of activated astrocytes in the perihematomal area was examined via immunohistochemistry at 1, 3, and 7 days post-ICH. The number of S100-positive cells increased at day 1 and remained elevated for 7 days in vehicle-treated mice, whereas Pyr3 administration significantly prevented the increase at days 1 and 3 (Supplementary Fig. 4).

Discussion

This study demonstrates for the first time that Pyr3, a selective TRPC3 inhibitor, ameliorated reactive astrogliosis and neurologic deficits resulting from collagenase and autologous blood infusion-induced ICH, whereas the drug did not affect hematoma formation. In addition, delayed administration of Pyr3 after the onset of brain injury was effective in both ICH models. These results suggest that Pyr3 can improve neuropathological outcomes after ICH in mice.

Emerging evidence suggests that activated astrocytes contribute to brain tissue damage after ICH. For example, matrix metalloproteinase (MMP) 9[20] and aquaporin (AQP) 4 and 9[21] are upregulated in activated astrocytes and stimulate the formation of edema after ICH. Moreover, activated astrocytes release S100B into the serum, which is significantly correlated with brain edema formation and hematoma volume in ICH[22] and hemorrhagic transformation in ischemia.[23] Furthermore, ICH-associated astrocyte reactivity is increased in aged compared with young rats,[5] while arundic acid, a specific inhibitor of S100B synthesis, mitigates delayed infarct expansion and neurologic deficits.[24] Thus, excessive activation of astrocytes is likely to influence clinical outcomes following stroke.

Our previous investigations demonstrated that thrombin-induced stimulation of proteinase-activated receptor-1 in astrocytes resulted in the opening of the TRPC3 channel as detected by Ca^{2+} imaging, the influxed Ca^{2+}-dependent activation of specific signaling molecules, *de novo* TRPC3 protein synthesis, feed-forward amplification of TRPC3 expression, and finally, functional astrogliosis *in vitro*.[11] These results imply

that thrombin leaked from ruptured blood vessels can activate astrocytes through TRPC3 channels *in vivo*. This hypothesis is strongly supported by our present results demonstrating that the selective TRPC3 inhibitor Pyr3 suppressed reactive astrogliosis and ameliorated functional recovery in mouse ICH model. Hence, suppression of astrocyte activation may ameliorate secondary injury after ICH.

It is however necessary to consider that Pyr3 treatment inhibits TRPC3 channels expressed in multiple cell types, including neurons, immune cells and endothelial cells. Accordingly, the inhibitory effect of Pyr3 against ICH might be attributed to a specific blockade of not only astrocyte but also monocyte/macrophage or neutrophil TRPC3 because these cells are mainly involved in the progression of secondary injury after ICH[4].

It has been reported that TRPC3 mediates ATP-induced vascular cell adhesion molecule 1 expression and resultant monocyte recruitment to the endothelium[25] and minocycline, an inhibitor of microglial/macrophage activation, can reduce the blood-brain barrier (BBB) damage and edema following ICH,[26] implying that Pyr3-mediated suppression of monocytes and endothelial cell functions via TRPC3 might contribute to the amelioration of ICH-induced brain injury. On the other hands, stimulation of phagocytosis in microglia/macrophage leads to the promotion of hematoma resolution, thereby the suppression of neuronal damage after ICH,[27] and macrophage TRPC3 contributes to survival signaling and efferocytic properties,[28] raising a fear that Pyr3 can exacerbate secondary injury after ICH to disrupt the physiological function of monocyte/macrophage. Furthermore, astrocytic accumulation

was comparatively early and peaked at day 1 after ICH, whereas microglial/macrophage accumulation was gradual and peaked at day 3-7, indicating that activation of astrocytes appears to precede that of microglial/macrophage in this ICH model. Taking into consideration that activated astrocytes can facilitate distant microglial activation in CNS disease,[29] the observed suppression of microglia/macrophages might be just a result of Pyr3-mediated suppression of astrocytes.

It has been reported that TRPC3 is also involved in the regulation of NADPH oxidase in the human neutrophil-like cell line[30] and neutrophil depletion reduces the BBB breakdown, axon injury, and astrocytic and microglia/macrophage responses after intracerebral hemorrhage,[31] raising the possibility that the inhibitory effect of Pyr3 may be due to a blockade of neutrophil TRPC3. Since our present data show that Pyr3 does not affect the infiltration of neutrophils after ICH, the observed effects of Pyr3 appear to be independent of neutrophils.

Meanwhile, TRPC3 is required to promote cerebellar granule neuron survival[32] and for metabotropic glutamate receptors-dependent synaptic transmission and motor coordination.[19] Therefore, the blockade of TRPC3 in neurons by Pyr3 may negatively impact neurological recovery post-ICH. Although Pyr3 alone did not show any neurological adverse effect in this study, development of a more selective, cell type-specific TRPC3 inhibitor may preserve the inhibitory actions against astrocytes while sparing neurons, further improving outcomes after ICH.

In this study, Pyr3 was administered through a combined intracerebroventricular/intraperitoneal route. Although intraperitoneal administration

alone weakly but significantly improved ICH-induced injury, the intracerebroventricular route was more effective, and the combined route was the most efficacious of all. These results are reminiscent of experiments with minocycline[33] and suggest that Pyr3 does not readily cross the BBB.

In the collagenase infusion ICH model (but not the autologous blood infusion model), the BBB was disrupted, and bleeding continued for up to 24 h.[34] Although hematoma formation was comparable in vehicle vs. Pyr3-treated mice subsequent to collagenase treatment, Pyr3 substantially improved collagenase-induced behavioral deficits and attenuated reactive astrogliosis. These results suggest that Pyr3 can ameliorate secondary brain injury stemming from ICH, without affecting the enzyme activity of collagenase or the integrity of the BBB.

In conclusion, the present findings indicate that thrombin released into the brain following ICH activates astrocytes via TRPC3, setting off a chain of events that ultimately induces neuronal death and neurological deficits. Thus, cell type-specific inhibitors of TRPC3 may constitute a novel class of therapeutic drugs for ICH.

Funding sources

This work was financially supported in part by a Grant-in-Aid for Scientific Research from the Ministry of Education, Culture, Sports, Science and Technology (MEXT) of Japan and by Grants from Ono Pharmaceutical Co., Ltd., the Research Foundation for Pharmaceutical Sciences, and Suzuken Memorial Foundation.

Disclosures

None.

References

1. Qureshi AI, Mendelow AD, Hanley DF. Intracerebral haemorrhage. *Lancet*. 2009;373:1632-1644.
2. Katsuki H. Exploring neuroprotective drug therapies for intracerebral hemorrhage. *J Pharmacol Sci.* 2010;114:366-378.
3. Matsushita H, Hijioka M, Hisatsune A, Isohama Y, Shudo K, Katsuki H. A retinoic acid receptor agonist Am80 rescues neurons, attenuates inflammatory reactions, and improves behavioral recovery after intracerebral hemorrhage in mice. *J Cereb Blood Flow Metab*. 2011;31:222-234.
4. Wang J, Doré S. Inflammation after intracerebral hemorrhage. *J Cereb Blood Flow Metab*. 2007;27:894-908.
5. Wasserman JK, Yang H, Schlichter LC. Glial responses, neuron death and lesion resolution after intracerebral hemorrhage in young vs. aged rats. *Eur J Neurosci*. 2008;28:1316-1328.
6. Barreto GE, Gonzalez J, Torres Y, Morales L. Astrocytic-neuronal crosstalk: implications for neuroprotection from brain injury. *Neurosci Res*. 2011;71:107-113.
7. Clapham DE. TRP channels as cellular sensors. *Nature*. 2003;426:517-524.
8. Ambudkar IS, Bandyopadhyay BC, Liu X, Lockwich TP, Paria B, Ong HL. Functional organization of TRPC-Ca^{2+} channels and regulation of calcium microdomains. *Cell Calcium*. 2006;40:495-504.
9. Trebak M, Vazquez G, Bird GS, Putney JW Jr, The TRPC3/6/7 subfamily of cation channels. *Cell Calcium*. 2003;33:451-461.

10. Nakao K, Shirakawa H, Sugishita A, Matsutani I, Niidome T, Nakagawa T et al. Ca2+ mobilization mediated by transient receptor potential canonical 3 is associated with thrombin-induced morphological changes in 1321N1 human astrocytoma cells. *J Neurosci Res.* 2008;86:2722-2732.
11. Shirakawa H, Sakimoto S, Nakao K, Sugishita A, Konno M, Iida S, et al. Transient receptor potential canonical 3 (TRPC3) mediates thrombin-induced astrocyte activation and upregulates its own expression in cortical astrocytes. *J Neurosci*. 2010;30:13116-13129.
12. Kitaoka T, Hua Y, Xi G, Hoff JT, Keep RF. Delayed argatroban treatment reduces edema in a rat model of intracerebral hemorrhage. Stroke. 2002;33:3012-3018.
13. Belayev L, Saul I, Curbelo K, Busto R, Belayev A, Zhang Y, et al. Experimental intracerebral hemorrhage in the mouse: histological, behavioral, and hemodynamic characterization of a double-injection model. *Stroke*. 2003;34:2221-2227.
14. Kiyonaka S, Kato K, Nishida M, Mio K, Numaga T, Sawaguchi Y, et al. Selective and direct inhibition of TRPC3 channels underlies biological activities of a pyrazole compound. *Proc Natl Acad Sci U S A.* 2009;106:5400-5405.
15. Kim MS, Lee KP, Yang D, Shin DM, Abramowitz J, Kiyonaka S, et al. Genetic and pharmacologic inhibition of the Ca2+ influx channel TRPC3 protects secretory epithelia from Ca2+-dependent toxicity. *Gastroenterology.* 2011;140:2107-2115.
16. Rynkowski MA, Kim GH, Komotar RJ, Otten ML, Ducruet AF, Zacharia BE, et al. A mouse model of intracerebral hemorrhage using autologous blood infusion. *Nat Protoc*. 2008;3:122-128.

17. Clark W, Gunion-Rinker L, Lessov N, Hazel K. Citicoline treatment for experimental intracerebral hemorrhage in mice. *Stroke*. 1998 ;29:2136-2140.
18. Austinat M, Braeuninger S, Pesquero JB, Brede M, Bader M, Stoll G, et al. Blockade of bradykinin receptor B1 but not bradykinin receptor B2 provides protection from cerebral infarction and brain edema. *Stroke*. 2009;40:285-293.
19. Hartmann J, Dragicevic E, Adelsberger H, Henning HA, Sumser M, Abramowitz J, et al. TRPC3 channels are required for synaptic transmission and motor coordination. *Neuron*. 2008;59:392-398.
20. Tejima E, Zhao BQ, Tsuji K, Rosell A, van Leyen K, Gonzalez RG, et al. Astrocytic induction of matrix metalloproteinase-9 and edema in brain hemorrhage. *J Cereb Blood Flow Metab*. 2007;27:460-468.
21. Sun Z, Zhao Z, Zhao S, Sheng Y, Zhao Z, Gao C, et al. Recombinant hirudin treatment modulates aquaporin-4 and aquaporin-9 expression after intracerebral hemorrhage in vivo. *Mol Biol Rep*. 2009;36:1119-1127.
22. Tanaka Y, Marumo T, Shibuta H, Omura T, Yoshida S. Serum S100B, brain edema, and hematoma formation in a rat model of collagenase-induced hemorrhagic stroke. *Brain Res Bull*. 2009;78:158-163.
23. Foerch C, Wunderlich MT, Dvorak F, Humpich M, Kahles T, Goertler M, et al. Elevated serum S100B levels indicate a higher risk of hemorrhagic transformation after thrombolytic therapy in acute stroke. *Stroke*. 2007;38:2491-2495.
24. Tateishi N, Mori T, Kagamiishi Y, Satoh S, Katsube N, Morikawa E, et al. Astrocytic activation and delayed infarct expansion after permanent focal ischemia

in rats. Part II: suppression of astrocytic activation by a novel agent (R)-(-)-2-propyloctanoic acid (ONO-2506) leads to mitigation of delayed infarct expansion and early improvement of neurologic deficits. *J Cereb Blood Flow Metab*. 2002;22:723-734.

25. Smedlund K, Bah M, Vazquez G. On the role of endothelial TRPC3 channels in endothelial dysfunction and cardiovascular disease. *Cardiovasc Hematol Agents Med Chem*. 2012;10:265-274.
26. Wasserman JK, Schlichter LC. Minocycline protects the blood-brain barrier and reduces edema following intracerebral hemorrhage in the rat. *Exp Neurol*. 2007;207:227-237.
27. Zhao X, Sun G, Zhang J, Strong R, Song W, Gonzales N. et al. Hematoma resolution as a target for intracerebral hemorrhage treatment: role for peroxisome proliferator-activated receptor gamma in microglia/macrophages. *Ann Neurol*. 2007;61:352-362.
28. Tano JY, Smedlund K, Lee R, Abramowitz J, Birnbaumer L, Vazquez G. Impairment of survival signaling and efferocytosis in TRPC3-deficient macrophages. *Biochem Biophys Res Commun*. 2011;410:643-647.
29. Liu W, Tang Y, Feng J. Cross talk between activation of microglia and astrocytes in pathological conditions in the central nervous system. *Life Sci*. 2011;89:141-146.
30. Bréchard S, Melchior C, Plançon S, Schenten V, Tschirhart EJ. Store-operated Ca2+ channels formed by TRPC1, TRPC6 and Orai1 and non-store-operated channels formed by TRPC3 are involved in the regulation of NADPH oxidase in HL-60

granulocytes. *Cell Calcium*. 2008;44:492-506.

31. Moxon-Emre I, Schlichter LC. Neutrophil depletion reduces blood-brain barrier breakdown, axon injury, and inflammation after intracerebral hemorrhage. *J Neuropathol Exp Neurol*. 2011;70:218-235.
32. Jia Y, Zhou J, Tai Y, Wang Y. TRPC channels promote cerebellar granule neuron survival. *Nat Neurosci.* 2007;10:559-567.
33. Xue M, Mikliaeva EI, Casha S, Zygun D, Demchuk A, Yong VW. Improving outcomes of neuroprotection by minocycline: guides from cell culture and intracerebral hemorrhage in mice. *Am J Pathol*. 2010;176:1193-1202.
34. MacLellan CL, Silasi G, Poon CC, Edmundson CL, Buist R, Peeling J, et al. Intracerebral hemorrhage models in rat: comparing collagenase to blood infusion. *J Cereb Blood Flow Metab*. 2008;28:516-525.

Figure Legends

Figure 1. Effect of Pyr3 on hematoma formation and neurological deficits in collagenase infusion ICH model mice. A, structural formula of Pyr3 and representative images of coronal sections obtained 6 h after collagenase injection showing similarly-sized hematomas in vehicle and Pyr3-treated mice. B–D, summarized data of neurological deficits, as assessed by the NDS (B), rotarod test (C), and rope grip test (D). Pyr3 was administered intracerebroventricularly (20 nmol) and intraperitoneally (40 mg/kg twice per day). n = 5–6; *P < 0.05, ***P < 0.001 vs. vehicle.

Figure 2. Effect of Pyr3 on injury volume and edema after collagenase-induced ICH. A–B, representative images of Nissl-stained coronal sections obtained 3 days after collagenase injection in vehicle-treated mice (A) and Pyr3-treated mice (B). C, summarized data of injury volume (dashed line in panels A and B). D, summarized data of hemispheric enlargement in the ipsilateral compared with the contralateral hemisphere. Pyr3 was administered intracerebroventricularly (20 nmol) and intraperitoneally (40 mg/kg twice per day). n = 6–9; ***P < 0.001 vs. vehicle.

Figure 3. Dose-dependent effects of Pyr3 on neurological deficits and brain injury at 3 days after collagenase-induced ICH. Summarized data of neurological deficits, as assessed by the NDS (A), rotarod test (B), rope grip test (C), and hemorrhagic injury volume (D). Pyr3 was administered intracerebroventricularly (i.c.v., 1, 10, or 20 nmol) and intraperitoneally (i.p., 2, 20, or 40 mg/kg twice per day). n = 4; *P < 0.05, **P <

0.01, ***P < 0.001 vs. vehicle.

Figure 4. Therapeutic time window of Pyr3 effects on neurological deficits and brain injury at 3 days after collagenase-induced ICH. Summarized data of neurological deficits, as assessed by the NDS (A), rotarod test (B), rope grip test (C), and hemorrhagic injury volume (D). Pyr3 was administered intracerebroventricularly (i.c.v., 20 nmol) and intraperitoneally (i.p., 40 mg/kg twice per day). n = 5–6; *P < 0.05, ***P < 0.001 vs. vehicle.

Figure 5. Inhibitory effect of Pyr3 on the number of astrocytes in the perihematomal area of collagenase-induced ICH mice. A, representative images of S100-positive cells. B, summarized data of the number of S100-positive cells. Pyr3 was administered intracerebroventricularly (20 nmol) and intraperitoneally (40 mg/kg twice per day). n = 5–8; *P < 0.05 vs. vehicle.

Figure 6. Effect of Pyr3 on autologous blood-induced ICH injury. A, representative images of coronal sections obtained 6 h after blood infusion showing similarly-sized hematomas in vehicle and Pyr3-treated mice. B, schematic representation of the experimental schedule (upper left) and summarized data of neurological deficits, as assessed by the NDS (upper right), rotarod test (lower left), and rope grip test (lower right). C, therapeutic time window of Pyr3. Schematic representation of the experimental schedule (upper left) and summarized data of neurological deficits, as

assessed by the NDS (upper right), rotarod test (lower left), and rope grip test (lower right). Pyr3 was administered intracerebroventricularly (i.c.v., 20 nmol) and intraperitoneally (i.p., 40 mg/kg twice per day). n = 5–8; **P < 0.01, ***P < 0.001 vs. vehicle.

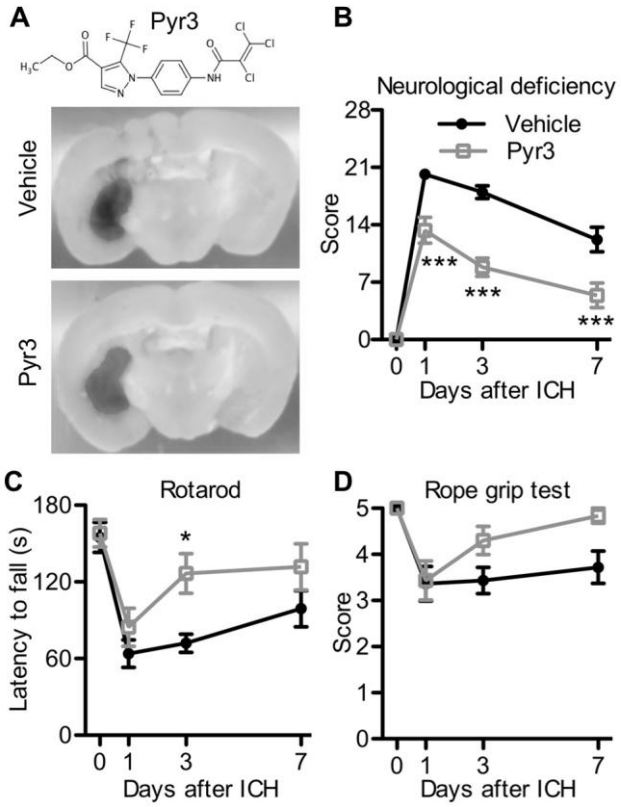

Munakata et al., 2013

Fig. 1

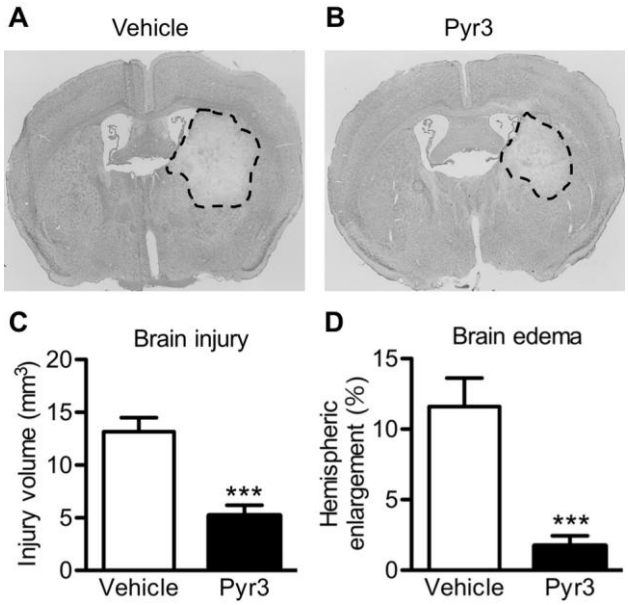

Munakata et al., 2013

Fig. 2

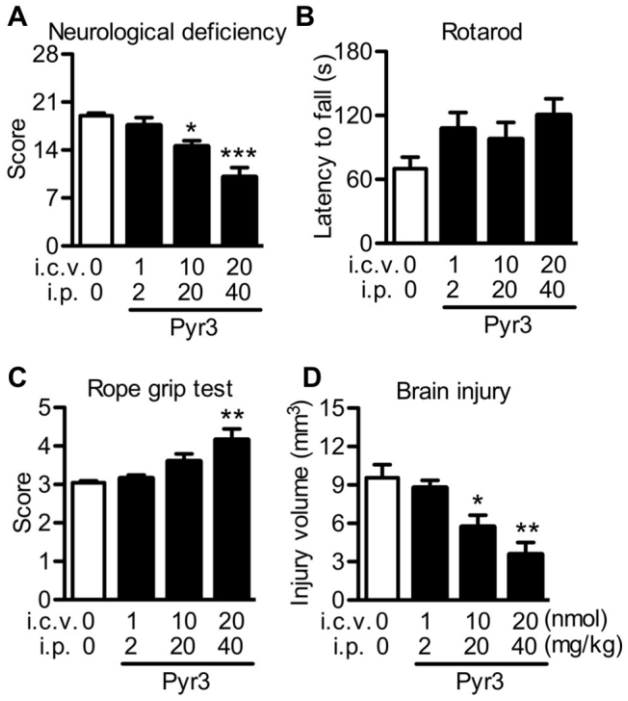

Munakata et al., 2013

Fig. 3

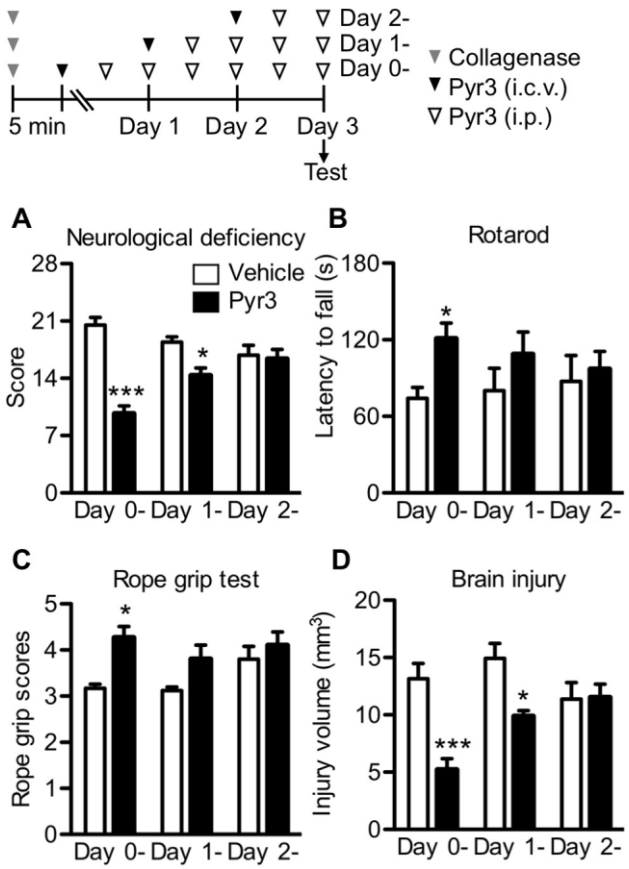

Munakata et al., 2013

Fig. 4

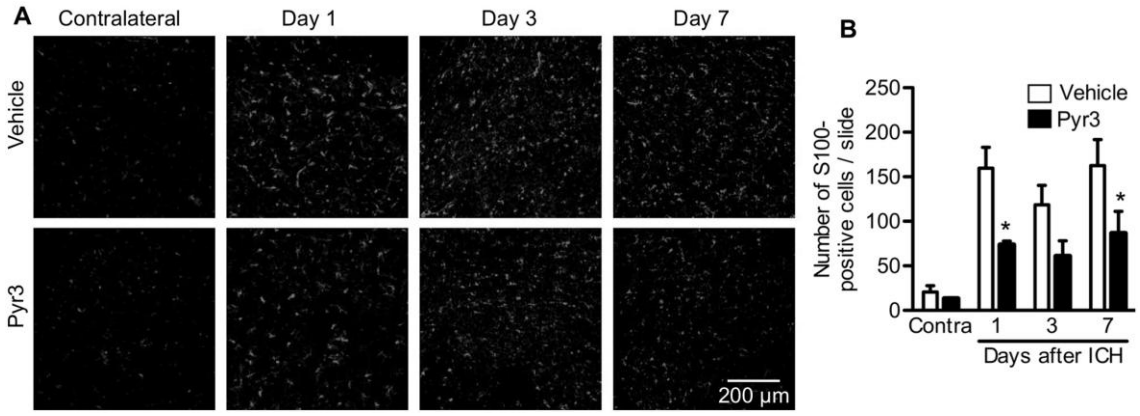

Munakata et al., 2013

Fig. 5

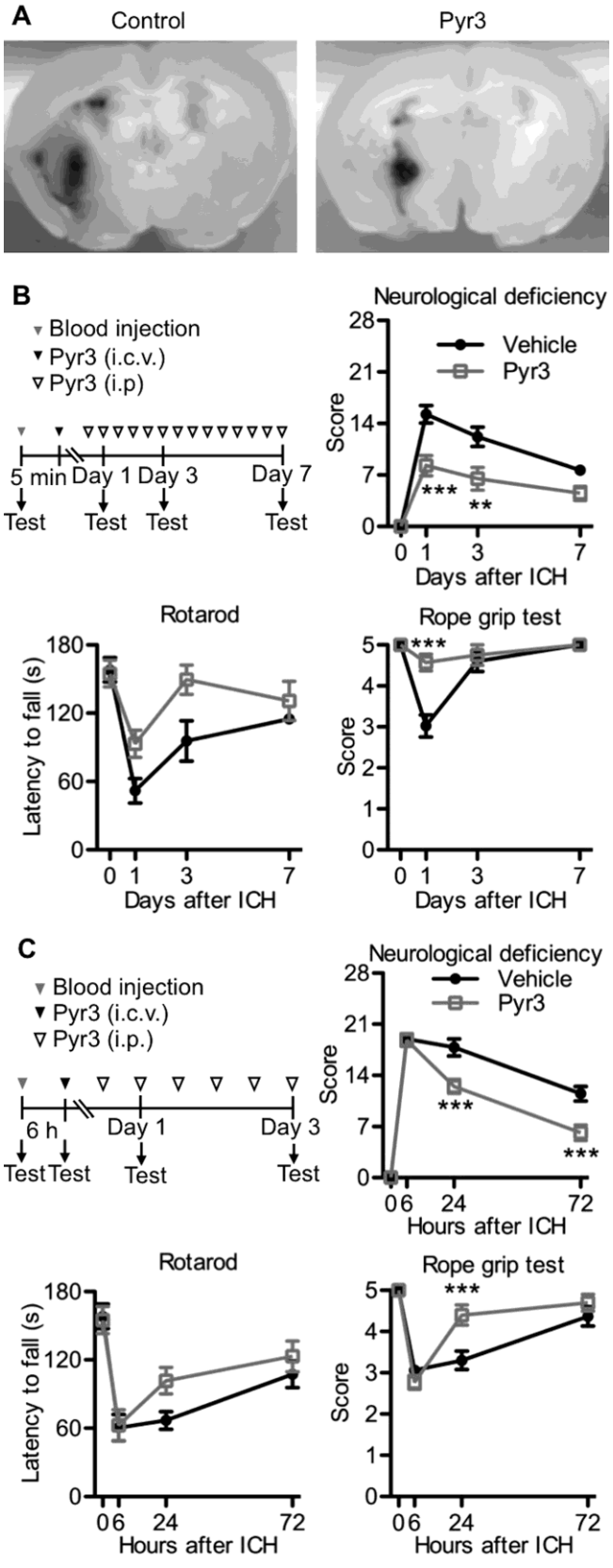

Munakata et al., 2013 Fig. 6

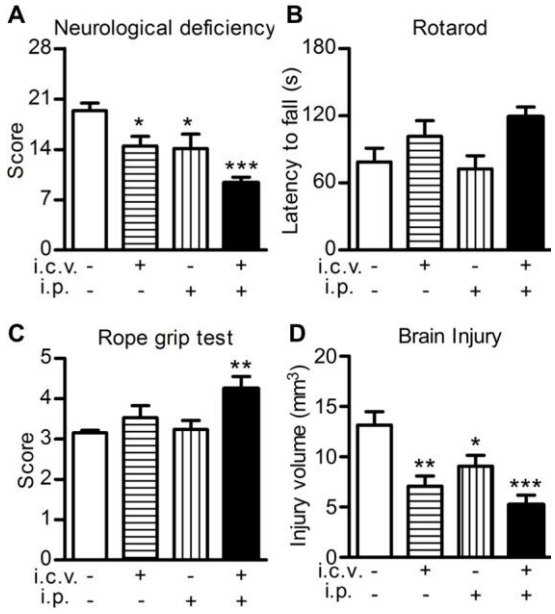

Munakata et al., 2013

Supplemental Fig. 1

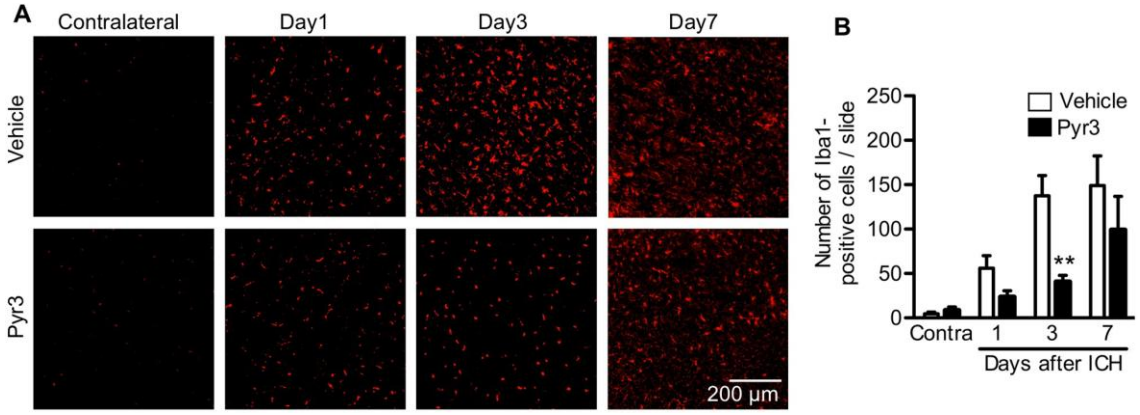

Supplemental Fig. 2

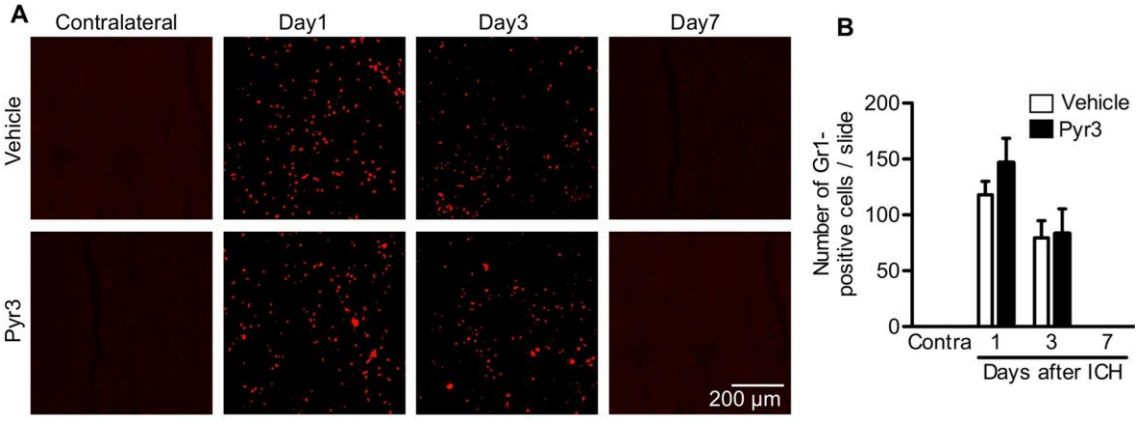

Supplemental Fig. 3

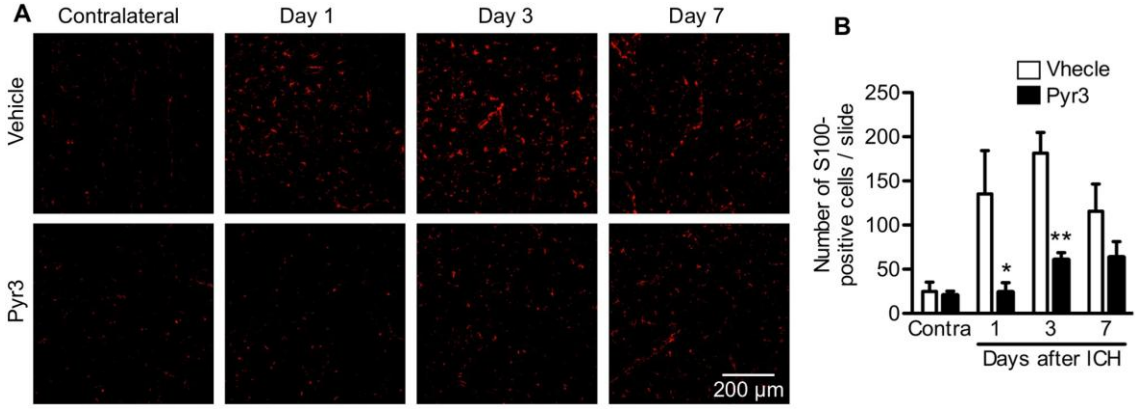

Supplemental Fig. 4

Supplemental Figure legends

Supplementary Figure 1. Effect of different routes of Pyr3 administration on ICH-induced injury at 3 days after collagenase injection. A–C, summarized data of neurological deficits, as assessed by the NDS (A), rotarod test (B), rope grip test (C), and hemorrhagic injury volume (D). Pyr3 was administered intracerebroventricularly (i.c.v., 20 nmol) and/or intraperitoneally (i.p., 40 mg/kg twice per day). n = 4; *P < 0.05, **P < 0.01, ***P < 0.001 vs. vehicle.

Supplementary Figure 2. Inhibitory effect of Pyr3 on the number of microglia/macrophages in the perihematomal area of collagenase-induced ICH mice. A, representative images of Iba1-positive cells. B, summarized data of the number of Iba1-positive cells. Pyr3 was administered intracerebroventricularly (20 nmol) and intraperitoneally (40 mg/kg twice per day). n = 6–7; **P < 0.01 vs. vehicle.

Supplementary Figure 3. Null effect of Pyr3 on the number of neutrophils in the hematomal area of collagenase-induced ICH mice. A, representative images of Gr1-positive cells. B, summarized data of the number of Gr1-positive cells. Pyr3 was administered intracerebroventricularly (20 nmol) and intraperitoneally (40 mg/kg twice per day). n = 3–5.

Supplementary Figure 4. Inhibitory effect of Pyr3 on the number of astrocytes in the perihematomal area of autologous blood-induced ICH mice. A, representative images of S100-positive cells. B, summarized data of the number of S100-positive cells. Pyr3 was

administered intracerebroventricularly (i.c.v., 20 nmol) and intraperitoneally (i.p., 40 mg/kg twice per day). n = 3–6; *P < 0.05, **P < 0.01 vs. vehicle.